



IJITCE

ISSN 2347- 3657

International Journal of Information Technology & Computer Engineering

www.ijitce.com



Email : ijitce.editor@gmail.com or editor@ijitce.com

ANALYSIS OF THE SMALL SIGNAL STABILITY OF THE POWER SYSTEM CONNECTED WITH WIND GENERATORS

K.Hanumaji¹, S.P.Vijayaragavan^{2*}

Research Scholar¹, Associate Professor²

Bharath Institute of Higher Education and Research^{1,2}

ABSTRACT

The main objective of this thesis is to study and analyze the small signal stability of the power system connected with wind generators, as the power generation using wind generators has gained importance in the recent days. Here, direct drive permanent magnet synchronous generator is considered in the investigation, and the small signal model is determined to survey the little unsettling influence steadiness. The eigen value examination researches the dynamic conduct of Power system under diverse modes. Thusly, by utilizing eigen esteem examination, the connection between the modes and the state variables are acquired. Along these lines by changing the controller parameters their impact on the eigen qualities are considered. The outcome demonstrates that the system security can be enhanced by appropriate tuning of both generator side and grid side converter controller parameters. Small signal model is developed for a grid connected PMSG based WECS. Eigen value analysis is performed for 3 machine nine 9 bus system using MATLAB/SIMULINK.

I. INTRODUCTION

The availability of electrical energy is a necessity for the functioning of modern societies. The energy consumption is increasing enormously in recent years, due to massive industrialization. The risks of shortage of fossil matters and their effects on the climatic change emphasis the use of alternate resource (renewable energy)[1-4].

The various available renewable resources are solar, hydro, wind etc. The generation of electrical power from wind farms is developing rapidly with worldwide installed capacity. Currently India stands fifth in the production of electricity from wind farms after China, USA, Germany, and Spain. The installed capacity in India is 16,000 MW.

Besides, of its advantage wind energy generation also has its disadvantages such as complexity, cost, and instability of wind speed. The cost disadvantage is reduced by subsidies from Government as

they are likely to promote the **green** power generation. On the other hand, cost of wind power is relatively lower when compared to other renewable energy resources[5-9].

The conduct of power system is primarily dictated by the conduct and communication of generators associated with it. At the point when the infiltration of wind production expands its impact on power system likewise increments. In this proposition, the impact of network associated variable rate wind vitality transformation system on the dependability of power system is considered[10-15].

II. MODELLING OF POWER SYSTEM COMPONENTS FOR STABILITY ANALYSIS

Dynamic model of grid connected wind energy conversion system is required to achieve knowledge about ongoing change in the system due to increasing wind energy penetration. This chapter deals with the mathematical modelling of power system consisting of differential and algebraic equations representing the models of system components including synchronous generators, loads[16-19].

WIND TURBINE MODEL

The simple streamlined model is utilized to speak to the turbine, which depends on the power coefficient, C_p versus the tip speed proportion λ , typically given by the maker. The power extricated from the wind is given by

$$T_m = \frac{\rho A V^3 C_p}{2\omega_r S_b} \quad (2.1)$$

The tip speed ratio is given by

$$\lambda = \frac{\omega_r R}{V} \quad (2.2)$$

A general functional representation of C_p is given by Lubosny (2003) as,

$$C_p = C_1(C_2 h - C_3 \beta - C_4) e^{-C_5 h} \quad (2.3)$$

Where,

$$h = \frac{1}{\lambda + 0.08\beta} - \frac{0.035}{\beta^3 + 1} \quad (2.4)$$

C_1 to C_6 are constants. The C_p versus λ curve is provided by the manufacturer. The constants C_1 to C_6 are computed for particular turbines using the procedure given by Heier (1998).

MODEL OF SYNCHRONOUS GENERATORS

The synchronous generator representation considers the excitation winding on the d-axis and a damper winding on the q-axis. Here for stability study Type 1A model of synchronous generators are considered[20-24].

The differential equations of synchronous generators

$$\frac{d\delta_i}{dt} = \omega_i - \omega_s \quad (2.5)$$

$$\frac{2H_i}{\omega_s} \frac{d\omega_i}{dt} = T_{Mi} - T_{ei} - D_i(\omega_i - \omega_s) \quad (2.6)$$

$$T'_{doi} \frac{dE'_{qi}}{dt} = -E'_{qi} - (X_{di} - X'_{di})I_{di} + E_{fdi} \quad (2.7)$$

$$T'_{qoi} \frac{dE'_{di}}{dt} = -E'_{di} + (X_{qi} - X'_{qi})I_{qi} \quad (2.8)$$

$$T_{ei} = E'_{di} I_{di} + E'_{qi} I_{qi} + (X'_{qi} - X'_{di}) \quad (2.9)$$

The stator algebraic equations are represented as follows

$$E'_{di} - V_i \sin(\delta_i - \theta_i) - R_{si} I_{di} + X'_{qi} I_{qi} = 0$$

$$E'_{qi} - V_i \cos(\delta_i - \theta_i) - R_{si} I_{qi} - X'_{di} I_{di} = 0$$

$$(2.10)$$

MODEL OF INDUCTION GENERATOR

The induction generator is spoken to by method for understood third order model. Utilizing again generator current convention, the electric torque of the induction machine is $T_{ei} = E'_{di} I_{di} + E'_{qi} I_{qi}$

$$(2.12)$$

$$\frac{dE'_r}{dt} = -\frac{[E'_r + (X_o - X')I_m]}{T'_o} - s\omega_s E'_m \quad (2.13)$$

$$\frac{dE'_m}{dt} = -\frac{[E'_m - (X_o - X')I_r]}{T'_o} + s\omega_s E'_r \quad (2.14)$$

$$\begin{aligned} E'_{ri} - V_i \cos(\theta_i) - RI_{di} + X'_{si} I_{mi} &= 0 \\ E'_{mi} - V_i \sin(\theta_i) - R_{si} I_{mi} - X'_{si} I_{ri} &= 0 \end{aligned} \quad (2.15)$$

A squirrel-cage induction machine connected to an AC power source of appropriate voltage can operate either as a motor or as a generator. The terminal voltage applied to the machine produces lagging magnetizing current, which in turn results in the rotating magnetic field within the air gap for both motoring and generating action. When the motor is loaded, current flows in short circuited rotor due to the rotor EMF and the motor runs at sub-synchronous speed[25-29].

When the induction machine runs at super-synchronous speed, a voltage is induced in the rotor in phase opposition to the EMF induced because of reversal of relative speed. The component of the stator current, which balances the rotor MMF, also reverses. The stator current now consists of magnetizing current as before and a component in phase opposition to the stator applied voltage. Thus the machine becomes an induction generator with external excitation. The induction generator can be represented by the well-known equivalent circuit shown in Fig 2.1.

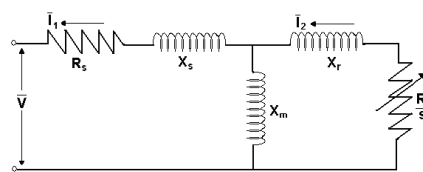


Fig 2.1 Steady state equivalent circuit of induction generator

From Fig2.1, the current I_1 can be written as,

$$\bar{I}_1 = \frac{\bar{V}}{(R_s + R_e) + j(X_s + X_e)} \quad (2.16)$$

$$R_e + jX_e = \frac{jX_m \left(\frac{R_r}{s} + jX_r \right)}{\frac{R_r}{s} + j(X_m + X_r)} \quad (2.17)$$

The per-unit active power transferred from the rotor to the stator through air gap, called air gap power, is readily calculated from the equivalent circuit as,

$$P_g = I_2^2 \frac{R_r}{s} \quad (2.18)$$

$$P_e = I_2^2 \frac{R_r}{s} (1-s) \quad (2.19)$$

$$\tau_e(V, s) = \frac{V^2 X_m^2 \frac{R_r}{s}}{\left[\left(R_x + \frac{R_r}{s} \right)^2 + (X_x + X_r)^2 \right] \left[R_s^2 + (X_s + X_m)^2 \right]} \quad (2.20)$$

Where,

$$R_x + jX_x = \frac{jX_m(R_s + jX_r)}{R_s + j(X_s + X_m)} \quad (2.21)$$

MODEL OF PMSG

Using Source convention, voltage equations of PMSG in d-q reference frame (q-axis leads d-axis in the direction of rotation) is

$$V_{ds}^{\phi} + R_s i_{ds}^{\phi} + \omega \psi_{qs}^{\phi} = 0 \quad (2.22)$$

$$V_{qs}^{\phi} + R_s i_{qs}^{\phi} + \omega \psi_{ds}^{\phi} = 0 \quad (2.23)$$

The flux linkage equations of PMSG is

$$\psi_{qs}^{\phi} = -L_q i_{qs}^{\phi} \quad (2.24)$$

$$\psi_{ds}^{\phi} = \psi_f \quad (2.25)$$

The active and reactive power equations are given by

$$P_s = V_{ds}^{\phi} i_{ds}^{\phi} + V_{qs}^{\phi} i_{qs}^{\phi} \quad (2.26)$$

$$Q_s = V_{ds}^{\phi} i_{qs}^{\phi} - V_{qs}^{\phi} i_{ds}^{\phi} \quad (2.27)$$

MODEL OF DRIVE TRAIN

The rotor of wind turbine and generator are connected directly, so they can be expressed together by

$$\dot{\omega}_r = \frac{1}{H}(T_m - T_e) \quad (2.28)$$

$$\dot{\delta} = \omega_s(\omega_r - 1) \quad (2.29)$$

Where

H- Equivalent inertia time constant of whole drive train.

T_m - mechanical torque.

T_e - Electro-magnetic torque.

MODEL OF CONVERTERS AND THEIR CONTROLLERS

Here d-axis stator current i_{ds} is controlled to zero and q-axis stator current i_{qs} controlled to track the maximal input of the wind turbine torque(L.Yang et al 2010).

$$i_{ds}^{\varphi} = 0 \quad (2.30)$$

$$i_{qs}^{\varphi} = \frac{k_{pw}}{\psi_s}(\omega_{rref} - \omega_r) + X_w \quad (2.31)$$

$$\dot{X}_w = \frac{k_{pw}}{T_w}(\omega_{rref} - \omega_r) \quad (2.32)$$

EQUATIONS OF GRID SIDE CONTROLLER

When the direction of q-axis is aligned with the voltage vector, then $V_{dg}=0$.

$$P_g = V_{qg}^{\varepsilon} i_{qg}^{\varepsilon} \quad (2.33)$$

$$Q_g = V_{qg}^{\varepsilon} i_{dg}^{\varepsilon} \quad (2.34)$$

$$i_{dg}^{\varepsilon} = k_{pv}(V_{dcref} - V_{dc}) + X_v \quad (2.35)$$

$$i_{qg}^{\varepsilon} = k_{pl}(V_{tref} - V_t) + X_4 \quad (2.36)$$

$$\dot{X}_v = \frac{k_{pv}}{T_v}(V_{dcref} - V_{dc}) \quad (2.37)$$

$$\dot{X}_4 = \frac{k_{p1}}{T_4} (V_{tref} - V_t) \quad (2.38)$$

EQUATION OF DC LINK VOLTAGE

$$\dot{V}_{dc} = \frac{1}{C V_{dc}} (V_{qs}^{\varphi} i_{qs}^{\varphi} - V_{da}^{\varepsilon} i_{dg}^{\varepsilon}) \quad (2.39)$$

Where, C - Dc link capacitor.

INTERFACING WITH POWER SYSTEM

PMSG connected to 3 rd bus of 3 machine nine bus system through a transmission line and transformer. The voltage equation describing the interface with the external system can be written as

$$V_{da} = V_{dg} - L i_{qg} \quad (2.40)$$

$$V_{qa} = V_{qg} + L i_{dg} \quad (2.41)$$

Where, L is sum of transmission line and transformer inductance.

NETWORK MODEL

The system comparisons for generator buses are:

$$I_{di} V_i \sin(\delta_i - \theta_i) + I_{qi} V_i \cos(\delta_i - \theta_i) + P_{Li} - \sum_{k=1}^n V_i V_k Y_{ik} \cos(\theta_i - \theta_k - \alpha_{ik}) = 0 \quad (2.42)$$

$$I_{di} V_i \cos(\delta_i - \theta_i) - I_{qi} V_i \sin(\delta_i - \theta_i) + Q_{Li} - \sum_{k=1}^n V_i V_k Y_{ik} \sin(\theta_i - \theta_k - \alpha_{ik}) = 0 \quad (2.43)$$

Where i= 1: m no of machines.

The network equations for load buses are:

$$P_{Li} - \sum_{k=1}^n V_i V_k Y_{ik} \cos(\theta_i - \theta_k - \alpha_{ik}) = 0 \quad (2.44)$$

$$Q_{Li} - \sum_{k=1}^n V_i V_k Y_{ik} \sin(\theta_i - \theta_k - \alpha_{ik}) = 0 \quad (2.45)$$

Where i= m+1 to n no of buses.

III. SMALL SIGNAL MODEL OF POWER SYSTEM COMPONENTS

In this approach, the network equations are written in power balance form. Although equivalent to the current balance form, it has some extra features. The extended DAE system Jacobian also contains information about the load flow Jacobian.

SMALL SIGNAL MODEL FOR SYNCHRONOUS GENERATORS

Linearization of DAE power system model is carried out by adopting the concepts presented by Pai et al (2004). Linearising the differential Equations (2.5) to (2.9),

$$\dot{\Delta x} = A_1 \Delta x + A_2 \Delta I_g + A_3 \Delta \hat{V}_g + E \Delta U \quad (3.1)$$

Where $A_1 = \text{Diag}(A_{1i})$, $A_2 = \text{Diag}(A_{2i})$, $A_3 = \text{Diag}(A_{3i})$ and $E = \text{Diag}(E_i)$

$$A_{1i} = \begin{bmatrix} -\frac{D_i}{M_i} & 0 & -\frac{I_{qi0}}{M_i} & -\frac{I_{di0}}{M_i} & 0 \\ \omega_s & 0 & 0 & 0 & 0 \\ 0 & 0 & -\frac{1}{T'_{d0i}} & 0 & \frac{1}{T'_{d0i}} \\ 0 & 0 & 0 & -\frac{1}{T'_{q0i}} & 0 \\ 0 & 0 & 0 & 0 & \frac{-1}{T_A} \end{bmatrix}$$

$$A_{2i} = \begin{bmatrix} \frac{[(X'_d - X'_q)I_{d0} + E'_{q0}]}{M_i} & \frac{[(X'_d - X'_q)I_{q0} + E'_{d0}]}{M_i} \\ 0 & 0 \\ 0 & \frac{(X_d - X'_d)}{T'_{d0}} \\ \frac{(X_q - X'_q)}{T'_{q0}} & 0 \\ 0 & 0 \end{bmatrix}$$

$$A_{3i} = \begin{bmatrix} 0 & 0 \\ 0 & 0 \\ 0 & 0 \\ 0 & 0 \\ 0 & -\frac{1}{T_A} \end{bmatrix}$$

$$0 = B_1 \Delta x + B_2 \Delta I_g + B_3 \Delta \hat{V}_g$$

(3.2)

Where,

$$\Delta x^T_i = [\Delta \omega_i \quad \Delta \delta_i \quad \Delta E'_{qi} \quad \Delta E'_{di} \quad \Delta E_{fdi}]$$

$$\Delta I^T_{gi} = [\Delta I_{qi} \quad \Delta I_{di}]$$

$$\Delta \hat{V}_{gi}^T = [\Delta \theta_{gi} \quad \Delta V_{gi}]$$

$$\Delta \hat{V}_{li}^T = [\Delta \theta_{li} \quad \Delta V_{li}]$$

Where $B_1 = \text{Diag}(B_{1i})$, $B_2 = \text{Diag}(B_{2i})$, $B_3 = \text{Diag}(B_{3i})$

$$B_{1i} = \begin{bmatrix} 0 & V_{i0} \sin(\delta_{i0} - \theta_{i0}) & 1 & 0 & 0 \\ 0 & -V_{i0} \cos(\delta_{i0} - \theta_{i0}) & 0 & 1 & 0 \end{bmatrix}$$

$$B_{2i} = \begin{bmatrix} R_{si} & -X'_{qi} \\ X'_{di} & R_{si} \end{bmatrix}$$

$$B_{3i} = \begin{bmatrix} -V_{i0} \cos(\delta_{i0} - \theta_{i0}) & \sin(\delta_{i0} - \theta_{i0}) \\ V_{i0} \sin(\delta_{i0} - \theta_{i0}) & \cos(\delta_{i0} - \theta_{i0}) \end{bmatrix}$$

The network equations (2.42) and (2.45) are linearized to obtain

$$0 = C_1 \Delta x + C_2 \Delta I_g + C_3 \Delta \hat{V}_g + C_4 \Delta \hat{V}_l$$

$$0 = C_1 \Delta x + C_2 \Delta I_g + C_3 \Delta \hat{V}_g + C_4 \Delta \hat{V}_l$$

(3.3)

C_1 and C_2 are block diagonal matrices and $C_3, C_4, D_1,$ and D_2 are full matrices .The block diagonal

$$C_{1i} = \begin{bmatrix} 0 & I_{di0}V_{i0} \cos(\delta_{i0} - \theta_{i0}) & 0 & 0 & 0 \\ 0 & -V_{i0}I_{qi0} \sin(\delta_{i0} - \theta_{i0}) & 0 & 0 & 0 \end{bmatrix}$$

matrices are

$$C_{2i} = \begin{bmatrix} V_{i0} \sin(\delta_{i0} - \theta_{i0}) & V_{i0} \cos(\delta_{i0} - \theta_{i0}) \\ V_{i0} \cos(\delta_{i0} - \theta_{i0}) & -V_{i0} \sin(\delta_{i0} - \theta_{i0}) \end{bmatrix}$$

Since ΔI_g is not of interest, it can be eliminated from using (3.2) and (3.3).Using ΔI_g from (3.2) as

$$\Delta I_g = -B^{-1}_2 B_1 \Delta x - B^{-1}_2 B_3 \Delta \hat{V}_g \quad (3.4)$$

$$\begin{aligned} \dot{\Delta x} &= (A_1 - A_2 B^{-1}_2 B_1) \Delta x - (A_3 - A_2 B^{-1}_2 B_3) \Delta \hat{V}_g + E \Delta u \\ 0 &= (C_1 - C_2 B^{-1}_2 B_1) \Delta x - (C_3 - C_2 B^{-1}_2 B_3) \Delta \hat{V}_g + C_4 \Delta \hat{V}_l + \Delta S_{LG}(V) \\ 0 &= D_1 \Delta \hat{V}_g + D_2 \Delta \hat{V}_l + \Delta S_L(V) \end{aligned}$$

$S_{LG}(v)$ and $S_{Ll}(v)$ are specified then (3.6) is in DAE form with the state vector Δx and the algebraic

vectors ΔV_g and ΔV_l . They can be rewritten as

$$\begin{aligned} \dot{\Delta x} &= A'_1 \Delta x + A'_3 \Delta \hat{V}_g + E \Delta u \\ 0 &= C'_1 \Delta x + C'_3 \Delta \hat{V}_g + C'_4 \Delta \hat{V}_l \\ 0 &= D'_1 \Delta \hat{V}_g + D'_4 \Delta \hat{V}_l \end{aligned}$$

$$\dot{\Delta x} = A_{sys} \Delta x + E \Delta u$$

Where

$$A_{sys} = A'_1 - [A'_2 \ A'_3]^{-1} \begin{bmatrix} B_1 \\ C_1 \end{bmatrix}$$

The state space linear model is

$$\begin{bmatrix} \dot{\Delta x}_{sgi} \\ 0 \\ 0 \\ 0 \end{bmatrix} = \begin{bmatrix} A_{SGi} & 0 & A_2 & A_3 & A_4 \\ B_1 & B_2 & B_3 & B_4 \\ C_1 & C_2 & C_3 & \\ D_1 & D_2 & D_4 \end{bmatrix} \begin{bmatrix} \Delta x_{sgi} \\ \Delta x I_{d-q} \\ \hat{\Delta V}_{gi} \\ \hat{\Delta v}_l \end{bmatrix}$$

(3.7)

INCLUSION OF INDUCTION

GENERATOR

Linearising the differential Equations (2.12) to (2.14),

$$\frac{d\Delta E'_r}{dt} = -\frac{[\Delta E'_r - (X_o - X')\Delta I_m]}{T'_o} + s_0 \omega_s \Delta E'_m + \Delta \omega_r \omega_s E'_{m0}$$

$$\frac{d\Delta E'_m}{dt} = -\frac{[\Delta E'_m + (X_o - X')\Delta I_r]}{T'_o} - s_0 \omega_s \Delta E'_r - \Delta \omega_r \omega_s E'_{r0}$$

$$\frac{d\Delta \omega}{dt} = \frac{\Delta T_m}{2H} - \frac{\Delta T_e}{2H}$$

(3.8)

Linearising the stator algebraic Equations (2.15)

$$\begin{aligned} \Delta E'_r + X'_s \Delta I_m - R_1 \Delta I_r + V_{i0} \sin \theta_{i0} \Delta \theta_i - \cos \theta_i \Delta V_i &= 0 \\ \Delta E'_m - X'_s \Delta I_r - R_1 \Delta I_m - V_{i0} \cos \theta_{i0} \Delta \theta_i - \sin \theta_i \Delta V_i &= 0 \end{aligned}$$

(3.9)

The linearized state model is added to the state space model by defining

$$\Delta x_{IG} = [\Delta \omega_r \quad \Delta E'_r \quad \Delta E'_m]$$

(3.10)

And the resulting new state space model is shown in (3.11)

Thus, the subsystem model corresponding to ΔX_{IG} is added below ΔX_{SG} . This results in a new non-zero sub-matrix A_4 together with a block diagonal matrix A_{IG} .

$$\begin{bmatrix} \dot{\Delta x}_{sGi} \\ \dot{\Delta x}_{iGi} \\ 0 \\ 0 \\ 0 \end{bmatrix} = \begin{bmatrix} A_{SGi} & 0 & A_2 & A_3 & A_4 \\ 0 & A_{IG} & & & \\ B_1 & & B_2 & B_3 & B_4 \\ C_1 & & C_2 & C_3 & \\ D_1 & & D_2 & & D_4 \end{bmatrix} \begin{bmatrix} \Delta x_{sGi} \\ \Delta x_{iGi} \\ \Delta x_{I_{d-q}} \\ \hat{\Delta V}_{gi} \\ \hat{\Delta v}_l \end{bmatrix} \quad (3.11)$$

INCLUSION OF PMSG

Linearising the differential Equations (2.1) to (2.4) and (2.22) to (2.41),

The differential equations after linearisation

$$\frac{d\Delta \omega}{dt} = \frac{\Delta T_m}{2H} - \frac{\Delta T_e}{2H} \quad (3.12)$$

$$\frac{d\Delta \delta}{dt} = \omega_s \Delta \omega \quad (3.13)$$

$$\frac{d\Delta V_{dc}}{dt} = \frac{1}{CV_{dc0}} (V_{qs0}^\varphi i_{qs0}^\varphi - V_{da0}^\varepsilon i_{dg0}^\varepsilon) - \frac{\Delta V_{dc}}{CV_{dc0}^2} (V_{qs0}^\varphi \Delta i_{qs}^\varphi - V_{da0}^\varepsilon \Delta i_{dg}^\varepsilon + \Delta V_{qs0}^\varphi i_{qs0}^\varphi - \Delta V_{da0}^\varepsilon i_{dg0}^\varepsilon) \quad (3.14)$$

$$\frac{d\Delta X_w}{dt} = \frac{K_{pw}}{T_w} (-\Delta \omega) \quad (3.15)$$

$$\frac{d\Delta X_v}{dt} = \frac{K_{pv}}{T_v} (-\Delta V_{dc})$$

(3.16)

$$\frac{d\Delta X_4}{dt} = \frac{K_{p1}}{T_4} (-\Delta V)$$

(3.17)

The real and reactive power equations are given by

$$\Delta P_g = \Delta V_{da}^{\varepsilon} i_{dg0}^{\varepsilon} + \Delta i_{dg}^{\varepsilon} V_{da0}^{\varepsilon}$$

(3.18)

$$\Delta Q_g = -\Delta V_{da}^{\varepsilon} i_{qg0}^{\varepsilon} - \Delta i_{qg}^{\varepsilon} V_{da0}^{\varepsilon}$$

(3.19)

$$A_{PMSG} = \begin{bmatrix} K_{pw} + a_{11} & 0 & 0 & a_{14} & 0 & 0 \\ \frac{2H}{\omega_s} & 0 & 0 & 0 & 0 & 0 \\ a_{31} & 0 & a_{33} & a_{34} & a_{35} & a_{36} \\ a_{41} & 0 & 0 & 0 & 0 & 0 \\ 0 & 0 & a_{53} & 0 & 0 & 0 \\ 0 & 0 & 0 & 0 & 0 & 0 \end{bmatrix}$$

Where,

$$a_{11} = T_m \left[(\omega_{rpm} \times dC_p \times dh - d\lambda) - C_p \right]$$

(3.20)

$$a_{14} = \frac{-1}{2H}$$

(3.21)

$$a_{31} = \frac{-V_{qso}^{\phi} K_{pw} + I_{qso}^{\phi} R_s K_{pw}}{CV_{dco} \omega_s}$$

(3.22)

$$a_{33} = \frac{K_{pv} V_{dgo}^{\varepsilon}}{CV_{dco}} - \frac{V_{qso}^{\phi} i_{qso}^{\phi}}{CV_{dco}^2} + \frac{V_{dao}^{\varepsilon} i_{dgo}^{\varepsilon}}{CV_{dco}^2} \quad (3.23)$$

$$a_{34} = \frac{V_{qso}^{\varphi} - R_s i_{qso}^{\varphi}}{CV_{dc} \psi_s} \quad (3.24)$$

$$a_{35} = \frac{-V_{dgo}^{\varepsilon}}{CV_{dc}} \quad (3.25)$$

$$a_{36} = \frac{i_{dgo}^{\varepsilon} L}{CV_{dco}} \quad (3.26)$$

$$a_{41} = \frac{-K_{pw}}{T_w} \quad (3.27)$$

$$a_{53} = \frac{-K_{pv}}{T_v} \quad (3.28)$$

$$A_2 = \begin{bmatrix} 0 & 0 \\ 0 & 0 \\ 0 & a_{32} \\ 0 & 0 \\ 0 & 0 \\ 0 & a_{52} \end{bmatrix}$$

Where,

$$a_{32} = -\frac{i_{dgo}^{\varepsilon}}{CV_{dco}}(1+k_{p1}L) \quad (3.29)$$

$$a_{52} = \frac{-K_{p1}}{T_4} \quad (3.30)$$

$$D_1 = \begin{bmatrix} 0 & 0 & -K_{pv}V_{dao}^{\varepsilon} & 0 & V_{dao}^{\varepsilon} & -Li_{dgo}^{\varepsilon} \\ 0 & 0 & 0 & 0 & 0 & d_{24} \end{bmatrix}$$

Where, $d_{24} = i_{qgo}^\varepsilon L - V_{dao}^\varepsilon$

(3.31)

$$D_4 = \begin{bmatrix} 0 & (K_{p1}L+1)i_{dgo}^\varepsilon \\ 0 & d_{22} \end{bmatrix}$$

Where, $d_{22} = K_{p1}V_{dao}^\varepsilon - i_{qgo}^\varepsilon - K_{p1}i_{qgo}^\varepsilon L$

(3.32)

$$\Delta X_{PMSG} = [\Delta\omega \ \Delta\delta \ \Delta V_{dc} \ \Delta X_w \ \Delta X_v \ \Delta X_4]$$

(3.33)

And the resulting new state space model is shown in (3.34)

Thus, the subsystem model corresponding to ΔX_{PMSG} is added below ΔX_{SG+IG} . This results in a new non-zero sub-matrix A_4 together with a block diagonal matrix A_{PMSG} . The sub matrices D_1 and D_4 are modified to include the real and reactive power injections PMSG[30-38].

$$\begin{bmatrix} \dot{\Delta x}_{sg1} \\ \dot{\Delta x}_{igi} \\ \dot{\Delta x}_{PMSGi} \\ 0 \\ 0 \\ 0 \end{bmatrix} = \begin{bmatrix} A_{sg1} & 0 & 0 & A_2 & A_3 & A_4 \\ 0 & A_{igi} & 0 & & & \\ 0 & 0 & A_{PMSGi} & & & \\ B_1 & & & B_2 & B_3 & B_4 \\ C_1 & & & C_2 & C_3 & \\ D_1 & & & D_2 & & D_3 \end{bmatrix} \begin{bmatrix} \Delta X_{sg1} \\ \Delta X_{igi} \\ \Delta X_{PMSGi} \\ \Delta i_{d-q} \\ \Delta \hat{V}_{gi} \\ \Delta \hat{V}_l \end{bmatrix}$$

(3.34)

IV.RESULTS AND DISCUSSION

This Chapter presents the small signal stability analysis 3 machine 9 bus system consisting of two synchronous generators and one PMSG based WECS. Then one induction generator is included in the system.

Table 4.1. Load Flow results for inclusion of PMSG

BUS TYPE	VOLTAGE (in p.u)	P _G (in p.u)	Q _G (in p.u)	-P _L (in p.u)	-Q _L (in p.u)
Swing	1.040∠0.000	1.5403	0.2264	-	-
P-V	1.025∠0.0007	1.6300	0.0245	-	-
P-Q	1.039∠0.0025	-	-	0.0158	0
P-Q	1.031∠-0.0014	-	-	0	0
P-Q	1.0028∠-0.0024	-	-	1.25	0.5
P-Q	1.0202∠-0.0027	-	-	0.9	0.3
P-Q	1.0280∠-0.0010	-	-	0	0
P-Q	1.0193∠-0.0023	-	-	1	0.35
P-Q	1.039∠-0.0025	-	-	0	0

Table 4.2.
inclusion of PMSG

Eigenvalues for

MODES	EIGEN VALUES	OSCILLATION FREQUENCY	DAMPING RATIO
δ_3	0	0	0
δ_2, ω_2	-7.3571 +/- 52.5151i	8.3580	0.1387
δ_1, ω_1	-1.2196 +/- 17.6519i	2.8094	0.0689
V_{dc}, X_V	-2.6256 +/- 6.5253i	1.0385	0.3733
E_{d2}, X_4	-5.6816 +/- 3.1660i	0.5039	0.8735

E_{fd1}	-4.7928	0.4689	1.0000
E_{fd2}	-4.9511	0	1.0000
E_{q1}	-0.0510	0	1.0000
E_{q2}	-0.2995	0	1.0000
ω_3, X_W	-17.2717 +/-5.9178i	0.9418	0.9460
E_{d1}	-3.2258	0	1.0000

The system remains stable after suffering a small disturbance since all eigenvalues have negative real parts. Five complex conjugate eigen values represent the four oscillatory modes. The six negative real eigenvalues represent the three non-oscillatory modes.

Table 4.3.Participation Factor for inclusion of PMSG

MODES	EIGENVALUES	WITH DISTURBANCES														
0	0.2452	0.2452	0.2646	0.2646	0	0	0.0004	0.0004	0.0002	0	0	0	0	0	0	0
0	0.2451	0.2451	0.2644	0.2644	0	0	0.0004	0.0004	0.0002	0	0	0	0	0	0	0
0	0.0007	0.0007	0.0013	0.0013	0	0	0.0479	0.0479	0.0554	0.0007	1.0913	0.0445	0	0	0	0
0	0	0	0	0	0	0	0	0	0	0	0	0	0	0	0	1
0	0	0	0.0002	0.0002	0	0	0.0625	0.0625	1.2847	0.0724	0.1206	0.0011	0	0	0	0
0	0.2732	0.2732	0.2558	0.2558	0	0	0.0185	0.0185	0.0004	0.0047	0	0.0018	0	0	0	0
0	0.2727	0.2727	0.2553	0.2553	0	0	0.0166	0.0166	0.0004	0.004	0.0001	0.0028	0	0	0	0
0	0.0615	0.0615	0.0142	0.0142	0	0	0.0277	0.0277	0.0019	0.01	0.0535	0.8924	0	0	0	0
0	0.075	0.075	0.0431	0.0431	0.0001	0.0001	0.5512	0.5512	0.0141	0.0462	0.0002	0.054	0	0	0	0
0	0.0002	0.0002	0.0001	0.0001	0	0	0.0163	0.0163	0.0417	1.0078	0.0018	0.011	0	0	0	0
0	0	0	0	0	0	0	0	0	0	0	0	0	1.5426	1.5426	0	0
1	0	0	0	0	0	0	0	0	0	0	0	0	0	0	0	0
0	0	0	0	0	0.5391	0.5391	0.0002	0.0002	0	0	0	0	0	0	0	0
0	0	0	0	0	0	0	0	0	0	0	0	0	1.5426	1.5426	0	0
0	0	0	0	0	0.5392	0.5392	0.0003	0.0003	0	0	0	0	0	0	0	0
0	0.0021	0.0021	0.0013	0.0013	0.0003	0.0003	0.6402	0.6402	0.2041	0.0365	0.0123	0.004	0	0	0	0

Table 4.4 Effect of wind variation (For 5 m/s and 11.5 m/s)

		WIND SPEED 5 m/s	WIND SPEED 11.5 m/s
δ_3	0	0	0
δ_2, ω_2	-7.2238 +/-51.2405i	-7.3019 +/-52.2491i	-7.3185 +/-51.483i
δ_1, ω_1	-1.0759 +/-17.6667i	-1.2036 +/- 17.6471i	-1.0687 +/-17.685i
V_{dc}, X_V	-5.7949 +/- 4.3239i	-2.7721 +/- 6.4688i	-6.3001 +/- 3.851i
E_{d2}, X_4	-5.5550 +/- 3.0689i	-5.6896 +/- 3.1580i	-5.4845 +/- 2.893i;
E_{fd1}	-4.8276	-4.7945	-4.8419
E_{fd2}	-4.9476	-4.9512	-4.9438
E_{q1}	-0.0601	-0.0521	-0.0602
E_{q2}	-0.2847	-0.2974	-0.2852
ω_3, X_W	-17.2717 +/- 5.9178i	-16.9417 +/- 6.8053i	-17.2992 +/- 5.8369i
E_{d1}	-3.2258	-3.2258	-3.2258

INFERENCE FROM PARTICIPATION FACTOR MATRIX

The participation factor gives the role played by a state variable in a particular mode. It is measure of relative participation of a state variable.

Table 4.4 represents the Eigen values of PMSG with the effect of wind variation 5 m/s,11.5 m/s. The small signal stability analysis is performed for possible minimum (5 m/s) and maximum wind speed (11.5 m/s).The result shows that the damping ratio of mechanical mode SG 1 reduced by 11%. The damping ratio of electrical mode of PMSG increases by 53.8%.

Table 4.5. Load Flow results for inclusion of PMSG and Induction generator

BUS TYPE	VOLTAGE (in p.u)	P _G (in p.u)	Q _G (in p.u)	-P _L (in p.u)	- Q _L (in p.u)
Swing	1.040∠0.000	1.5403	0.2264	-	-
P-V	1.025∠0.0396	1.6300	0.0306	-	-
P-Q	1.0388∠-0.141	-	-	0.0158	0
P-Q	1.0308∠-0.0824	-	-	0	0.05
P-Q	1.0027∠-0.1393	-	-	1.25	0.5
P-Q	1.0201∠-0.1538	-	-	0.9	0.3

P-Q	1.0280∠-0.0572	-	-	0	0
P-Q	1.0193∠-0.1319	-	-	1	0.35
P-Q	1.0388∠-0.1419	-	-	0	0

Table 4.6. Eigenvalues for inclusion of PMSG and Induction generator

MODES	EIGEN VALUES	OSCILLATION FREQUENCY	DAMPING RATIO
δ_4	0	0	0
ω_2, E_m	-10.8513 +/- 8.330i	1.3259	0.6292
δ_1, ω_1	-0.5891 +/- 8.2051i	1.3059	0.0051
E_r	-9.5838	0	1.0000
V_{dc}, X_V	-2.6262 +/- 6.5251i	1.0385	0.1394
X_4, E_{fd1}, E_{fd2}	-3.2269 +/- 2.9459i	0.4689	0.5454
X_4, E_{d1}, E_{d2}	-3.6426	0	1.0000
E_{fd1}, E_{q1}	-3.0898 +/- 1.4465i	0.2302	0.8202
E_{q2}	-1.4786	0	1.0000
δ_1, δ_2	-0.0000	0	1.0000
$\delta_1, \omega_1, \delta_2, \omega_2$	-0.3474	0	1.0000
ω_4, X_W	-17.2717 +/- 5.917i	0.9418	0.8949
E_{d1}	-3.2258	0	1.0000

INFERENCE FROM EIGENVALUES

The system remains stable after suffering a small disturbance since all eigenvalues have negative real parts. Six complex conjugate eigen values represent the four oscillatory modes. The six negative real eigenvalues represent the three non-oscillatory modes.

Table 4.7.Participation Factor for inclusion of PMSG and Induction generator

0	0.0005	0.0005	0.1059	0.1059	0	0.0001	0.0001	0.0029	0.0029	0.0067	0.0036	0.0036	0.0017	0	0.7891	0	0	0
0	0.0005	0.0005	0.1057	0.1057	0	0.0001	0.0001	0.0028	0.0028	0.0063	0.0034	0.0034	0.0015	0.4812	0.3087	0	0	0
0	0	0	0.0004	0.0004	0.0003	0	0	0.236	0.236	0.1648	0.7113	0.7113	0.0179	0	0	0	0	0
0	0	0	0	0	0	0	0	0	0	0	0	0	0	0	0	0	0	1
0	0	0	0.0003	0.0003	0.0006	0	0	0.2939	0.2939	0.4176	0.9677	0.9677	0.0065	0	0	0	0	0
0	0.0003	0.0003	0.3964	0.3964	0	0.0001	0.0001	0.0125	0.0125	0.0346	0.0172	0.0172	0.0152	0	0.2125	0	0	0
0	0.0003	0.0003	0.3954	0.3954	0	0.0001	0.0001	0.0109	0.0109	0.0272	0.0137	0.0137	0.0072	0.4746	0.2653	0	0	0
0	0	0	0.0124	0.0124	0.0001	0	0	0.2835	0.2835	0.0622	0.2239	0.2239	0.847	0	0.0002	0	0	0
0	0	0	0.0166	0.0166	0.0005	0.0001	0.0001	0.0915	0.0915	0.6512	0.1787	0.1787	0.2675	0	0	0	0	0
0	0	0	0.0042	0.0042	0.0001	0	0	0.3473	0.3473	0.1659	0.3114	0.3114	0.3238	0	0	0	0	0
0	0.485	0.485	0	0	0.0342	0	0	0	0	0	0	0	0	0	0.0005	0	0	0
0	0.0205	0.0205	0	0	0.9684	0	0	0.0009	0.0009	0	0.0003	0.0003	0	0.0014	0.0015	0	0	0
0	0.5063	0.5063	0	0	0.0039	0	0	0	0	0.0001	0	0	0	0.0456	0.0471	0	0	0
0	0	0	0	0	0	0	0	0	0	0	0	0	0	0	0	1.5426	1.5426	0
1	0	0	0	0	0	0	0	0	0	0	0	0	0	0	0	0	0	0
0	0	0	0	0	0	0.539	0.539	0.0002	0.0002	0	0	0	0	0	0	0	0	0
0	0	0	0	0	0	0	0	0	0	0	0	0	0	0	0	1.5426	1.5426	0
0	0	0	0	0	0	0.5391	0.5391	0.0002	0.0002	0	0	0	0	0	0	0	0	0
0	0	0	0.0006	0.0006	0.0004	0.0004	0.0004	0.2571	0.2571	0.5726	0.2328	0.2328	0.2234	0	0	0	0	0

The participation matrix gives the role of state variables in particular modes. The state variables that influences the modes are shown in table 4.5.

OPTIMISED VALUES

Tuned Parameters values for inclusion of PMSG

$$K_{pw}=11.3112 \text{ p.u} \quad T_w=0.4941 \text{ sec}$$

$$K_{pv}=8.2219 \text{ p.u} \quad T_v=0.1641 \text{ sec}$$

$$K_{p1}=2.8264 \text{ p.u} \quad T_4=0.1587 \text{ sec}$$

Table 4.8.ImprovedEigenvalues for inclusion of PMSG

NO	EIGEN VALUES (*e0.02)	OSCILLATION FREQUENCY	DAMPING RATIO
1	0	0	0
2	-0.7506	0	1

3,4	-0.0738 +/- 0.5281i	8.4050	0.1384
5,6	-0.0124 +/- 0.1765i	2.81	0.0701
7,8	-0.0555 +/- 0.0397i	6.3	0.8133
9	-0.0661	0	1
10	-0.0473	0	1
11	-0.0496	0	1
12	-0.0005	0	1
13	-0.0030	0	1
14	-7.5328	0	1
15	-0.0201	0	1
16	-0.0323	0	1

Table 4.9.ImprovedEigenvalues for inclusion of PMSG and Induction generator

NO	EIGEN VALUES (*e0.02)	OSCILLATION FREQUENCY	DAMPING RATIO
1	0	0	0
2	-0.6913	0	1
3,4	-0.1085 +/- 0.0833i	1.33	0.7932
5,6	-0.0059 +/- 0.0820i	1.31	0.0718
7	-0.0959	0	1
8	-0.0688	0	1
9,10	-0.0267 +/- 0.0290i	0.46	0.6773
11,12	-0.0346 +/-0.0131i	0.21	0.9352
13	-0.0000	0	1
14	-0.0035	0	1
15	-0.0100	0	1
16	-0.0236	0	1
17	-7.0080	0	1
18	-0.0279	0	1
19	-0.0323	0	1

Tuned values for inclusion of PMSG and induction generator

$K_{pw} = 10.5359$ p.u $T_w = 0.3592$ sec

$K_{pv} = 7.6496$ p.u $T_v = 0.1591$ sec

$K_{pi} = 1.8919$ p.u $T_4 = 0.2298$ sec

REFERENCES

- [1] A. Tabesh R. Iravani, "Small-signal model and dynamic analysis of variable speed induction machine wind farms", IET Renew. Power Gener., Vol. 2, No. 4, pp. 215–227, 2008.
- [2] Feng Wu, Xiao-Ping Zhang, Ping Ju, "Modeling and Control of the Wind Turbine with the Direct Drive Permanent Magnet Generator Integrated to Power Grid", DRPT April Nanjing China, 2008.
- [3] G. Slootweg, H. Polinder, W.L. Kling, "Initialization of Wind Turbine Models in Power System Dynamics Simulations" IEEE Porto Power Tech Conference 10th -13th September, Portugal, 2001.
- [4] H. Huang C. Mao J. Lu D. Wang, "Small-signal modelling and analysis of wind turbine with direct drive permanent magnet synchronous generator connected to power grid" IET Renew. Power Gener., Vol. 6, Iss. 1, pp. 48–58, 2012.
- [5] IEEE TF report, "Proposed terms and definitions for power system stability," *IEEE Trans. on Power Appar. and Syst.*, Vol. PAS-101, pp.1894-1897, July, 1982.
- [6] L. Yang, G.Y. Yang Z. Xu, Z.Y. Dong K.P. Wong. Mal, "Optimal controller design of a doubly-fed Induction generator wind turbine system for small signal stability enhancement", IET Gener. Transm. Distrib., Vol. 4, Iss. 5, pp. 579–597, 2010.
- [7] M.A. Pai, D.P. Sen Gupta, K.R. Padiyar, "Small signal analysis of power systems", Narosa Publishing House.
- [8] Mayouf. Messaoud, Rachid. Abdessame, "Modeling and Optimization of Wind Turbine Driving Permanent Magnet Synchronous Generator", JJMIE Volume 5, Number 6, Dec. Pages 489 – 494, 2011.
- [9] M. E. Haque, K. M. Muttaqi and M. Negnevitsky, "Control of a Stand Alone Variable Speed Wind Turbine with a Permanent Magnet Synchronous Generator," IEEE Power and Energy Society General Meeting - Conversion and Delivery of Electrical Energy in the 21st Century, pp.1-9, 2008.

- [10] Peter W. Sauer, M.A. Pai, "Power System Dynamics and Stability", Pearson Education Pte. Ltd, 1998.
- [11] P. Kundur, "Power System Stability and Control", McGraw-Hill, inc., 1993.
- [12] P.M Anderson and A.A Fouad, "Power System Control and Stability", Iowa State University Press, Ames, Iowa, 1978.
- [13] R. Melício, V. M. F. Mendes, J. P. S. Catalão, "Transient Analysis of Variable-Speed Wind Turbines during a Converter Control Malfunction" the International Conference on Power Systems Transients (IPST) in Delft, the Netherlands, 2011.
- [14] R. Ramanujam, "Power System Dynamics", PHI Learning Private Limited, 2009.
- [15] Shuhui Li, Timothy A. Haskew Richard P. Swatloski, and William Gathings, "Optimal and Direct-Current Vector Control of Direct-Driven PMSG Wind Turbines" IEEE Transactions on Power Electronics, Vol. 27, No. 5, May, 2012.
- [16] Xiangyu Zhang, Yi Wang, Heming Li, "Control of PMSG-Based Wind Turbines to Damp the Power System Oscillations", IEEE PEDS, Singapore, December, 2011.
- [17] Y. Errami, M. Maaroufi, M. Ouassaid, "Modelling and Control Strategy of PMSG Based Variable Speed Wind Energy Conversion System", ICMCS, page no 1-6, April, 2011
- [18] Z. Lubosny, Wind Turbine Operation in Electric Power Systems - Advanced modelling, Springer Verlag, 2003.
- [19] S. Prakash, "Energy Conservation Through Standby Power Reduction," Middle-East Journal of Scientific Research, Vol. 19, No. 7, pp.990-994, January, 2014.
- [20] S. Prakash, "Modern Measures to Reduce the Impact of Lightning," Middle-East Journal of Scientific Research, Vol. 19, No. 7, pp.919-927, January, 2014.
- [21] P. Sivaramakrishnan and S. Prakash, "Optimum Location of Shunt Fact Devices for Transmission Line Compensation," International Journal of Scientific & Engineering Research, Vol. 5, No. 4, pp.169-173, April, 2014.
- [22] M. Krishna Kumar and S. Prakash, "Design and Implementation of a New Three-Phase Two-Switch ZVS PFC DCM Boost Rectifier," International Journal of Scientific Engineering and Research (IJSER), Vol. 2, No. 10, pp.14-24, October, 2014.

- [23] S. Vinod, S. Prakash and Dr. A. Kalirasu, "Study of SVM Based Controller for Grid Connected Wind Turbine," International Journal of Advanced Research in Electrical, Electronics and Instrumentation Engineering, Vol. 4, No. 4, pp.2079-2090, April, 2015.
- [24] Sengottuvel, P., Satishkumar, S., Dinakaran, D., Optimization of multiple characteristics of EDM parameters based on desirability approach and fuzzy modeling, Procedia Engineering, v-64, i-, pp-1069-1078, 2013.
- [25] Jayalakshmi, V., Gunasekar, N.O., Implementation of discrete PWM control scheme on Dynamic Voltage Restorer for the mitigation of voltage sag /swell, 2013 International Conference on Energy Efficient Technologies for Sustainability, ICEETS 2013, pp-1036-1040, 2013.
- [26] Kaliyamurthie, K.P., Parameswari, D., Udayakumar, R., QOS aware privacy preserving location monitoring in wireless sensor network, Indian Journal of Science and Technology, v-6, i-5, pp-4648-4652, 2013.
- [27] Sundararajan, M., Optical instrument for correlative analysis of human ECG and breathing signal, International Journal of Biomedical Engineering and Technology, v-6, i-4, pp-350-362, 2011.
- [28] Kaliyamurthie, K.P., Udayakumar, R., Parameswari, D., Mugunthan, S.N., Highly secured online voting system over network, Indian Journal of Science and Technology, v-6, i-SUPPL.6, pp-4831-4836, 2013.
- [29] Khanaa, V., Thooyamani, K.P., Saravanan, T., Simulation of an all optical full adder using optical switch, Indian Journal of Science and Technology, v-6, i-SUPPL.6, pp-4733-4736, 2013.
- [30] Raj, M.S., Saravanan, T., Srinivasan, V., A modified direct torque control of induction motor using space vector modulation technique, Middle - East Journal of Scientific Research, v-20, i-11, pp-1572-1574, 2014.
- [31] Kumaravel, A., Dutta, P., Application of Pca for context selection for collaborative filtering, Middle - East Journal of Scientific Research, v-20, i-1, pp-88-93, 2014.
- [32] Brintha Rajakumari, S., Nalini, C., An efficient data mining dataset preparation using aggregation in relational database, Indian Journal of Science and Technology, v-7, i-, pp-44-46, 2014.
- [33] Udayakumar, R., Khanaa, V., Saravanan, T., Saritha, G., Retinal image analysis using curvelet transform and multistructure elements morphology by reconstruction, Middle - East Journal of Scientific

Research, v-16, i-12, pp-1781-1785, 2013.

[34] Khanaa, V., Thooyamani, K.P., Using triangular shaped stepped impedance resonators design of compact microstrip quad-band, Middle - East Journal of Scientific Research, v-18, i-12, pp-1842-1844, 2013.

[35] Thamocharan, C., Prabhakar, S., Vanangamudi, S., Anbazhagan, R., Anti-lock braking system in two wheelers, Middle - East Journal of Scientific Research, v-20, i-12, pp-2274-2278, 2014.

[36] Vanangamudi, S., Prabhakar, S., Thamocharan, C., Anbazhagan, R., Design and fabrication of dual clutch, Middle - East Journal of Scientific Research, v-20, i-12, pp-1816-1818, 2014.

[37] Vanangamudi, S., Prabhakar, S., Thamocharan, C., Anbazhagan, R., Design and calculation with fabrication of an aero hydraulic clutch, Middle - East Journal of Scientific Research, v-20, i-12, pp-1796-1798, 2014.

[38] Saravanan, T., Raj, M.S., Gopalakrishnan, K., VLSI based 1-D ICT processor for image coding, Middle - East Journal of Scientific Research, v-20, i-11, pp-1511-1516, 2014.